

Internal MIMO Antenna Design for Multi-Band Mobile Handset Applications

Atta Ullah^{1,2}, Naser Ojaroudi Parchin³, Mohamed Abdul-Al¹, Henrique M. D. Santos², Chan Hwang See³, Yim Fun Hu¹, and Raed A. Abd-Alhameed¹

¹ Faculty of Engineering and Informatics, University of Bradford, Bradford, UK

² Department of Information systems, Minho's University, Azurém Campus 4800-058 Guimaraes, Portugal

³ School of Engineering and the Built Environment, Edinburgh Napier University, Edinburgh, UK

Abstract— In this research study, a new of 2×2 interior multi-band MIMO antenna is introduced for smartphone usages. The alignment of the antenna element contains a multi-mode monopole radiator with three L-shaped slits positioned at the border of the printed circuit board (PCB) of the cellular platform. The low-cost FR4 substrate is used for this new design with a total dimension of 60×135×0.5 mm³. For $S_{11} \leq -6$ dB, the antenna is covering the operational ranges of 0.79–0.92, 1.5–2.7, 3.5–3.85, and 5–9.5 GHz supporting IMT, PCS, UMTS, DCS, WLAN, LTE, and X bands. The premeditated MIMO antenna delivers appropriate gains different at frequency bands and worthy efficiencies, particularly at the upper bands. In addition, the considered ECC, DG, and TARC outcomes of the antenna are appropriate over the operational bands.

Keywords — Internal antenna, MIMO, monopole antenna, multi-band antenna, smartphone applications.

I. INTRODUCTION

In today's era, for cellular communication's MIMO expertise is the supreme encouraging skill to impact the essential transfer data rates [1-2]. Several antenna Element is required MIMO smartphone structure, which functions synchronously to attain structure diversity gain [3-4]. For new mobile technologies, multiband antenna schemes cover numerous ranges of cellular phone applications such as GPS, WIFI, GSM/LTE, etc. are extremely essential [5-7]. Nevertheless, planning multi-working operational band antennas in the narrow size of the smartphone central sheet is a substantial test for antenna designers. Between several MIMO antennas, microstrip antennas such as loop, slot, monopole radiators, and planar reversed-F antenna (PIFA) are other appropriate to be used in mobile handset systems due to their compressed shape, cheap price, manufacturability, and relaxed combination [8-10].

Although PIFA antennas are identical prevalent due to their structures such as multi-band and squeezed size features. Nevertheless, subsequently, PIFAs have extraordinary, pulverized level surface current characteristic, this kind of antenna is vastly delicate to user collaboration [11-12]. The anticipated antenna in this article is appropriate for the multi-mode application and it can cover numerous mobile terminals. The outline of the strategy is poised of dual multi-band antenna radiators positioned at upper plus lower edges of smartphone PCB. The antenna component is

comprising a monopole radiator with three L-shaped slits. A detached feeding practice is active for the antenna elements [13-14]. The projected antenna conquers minor zone and illustrates respectable radiation features which make it appropriate for handheld devices functioning at long-term evolution (LTE), personal communication system (PCS), X-band frequency spectrums, universal mobile telecommunications service (UMTS), digital communication system (DCS), wireless local area network (WLAN) and international mobile telecommunications (IMT). The CST software is utilized to examine the proposed project things [15].

II. MULTI-BAND MONOPOLE ANTENNA DESIGN

The outline along with projected parameters of the individual component smartphone antenna is characterized in Fig. 1. It comprises a monopole radiator with three L-shaped slits. The antenna is accomplished on a low-priced FR-4 with particulars of loss tangent=0.025, permittivity=4.4, and thickness of 0.5 mm. The constraint principles of the antenna are registered in Table 1.

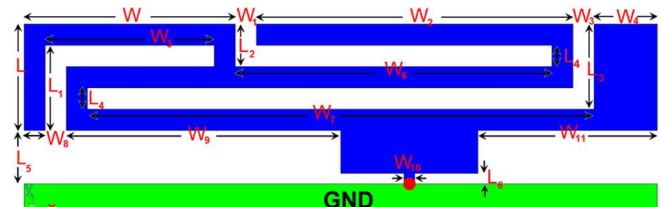


Fig. 1. Design details of the antenna.

TABLE. I PARAMETER VALUES OF THE DESIGN

Parameter	W	L	W ₁	L ₁	W ₂	L ₂ =L ₄	W ₃
Value (mm)	20	10	2	8	30	4	2
Parameter	L ₃	W ₄	W ₅	L ₅	W ₆	L ₆	W ₇
Value (mm)	8	6	16	5	30	1	48
Parameter	W ₈	W ₉	W ₁₀	W ₁₁	W _x	L _x	W _{x1}
Value (mm)	2	26	1	17	105	60	15

The return loss of the antenna is managed in Figs. 2 and 3. As seen, for $S_{11} \leq -6$ dB, the planned antenna covers the operational bands of 0.79–0.92, 1.5–2.7, 3.5–3.85, and 5–9.5 GHz. However, for $S_{11} \leq -10$ dB, the antenna operates at 0.84-0.9 GHz, 1.7-2.4, 3.55-3.7, and 5.2-9 GHz.

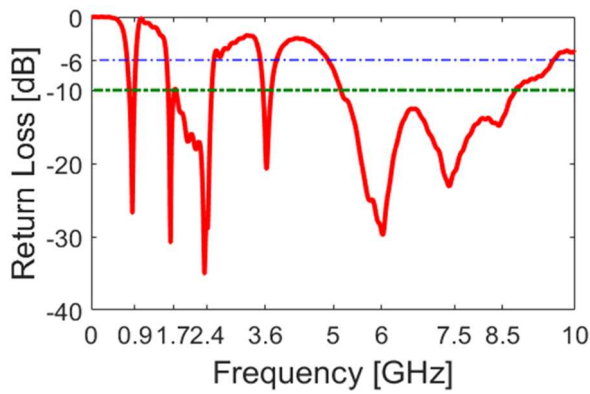


Fig. 2. S_{11} characteristic of the planned antenna.

In order to analyse the working principle of the proposed multi-band antenna design, the design evolution and simulated return loss result of each antenna are presented in Fig. 3 and discussed in Fig. 4. As illustrated in Fig. 4, by adding three modified L-shaped slits in the configuration of the monopole antenna (from Ant. 1 to Ant. 4), not only new resonances are generated, but also the impedance bandwidth of the design has been improved [16].

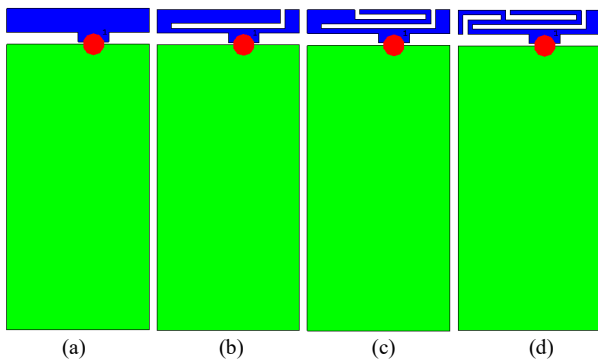


Fig. 3. Design evolution; (a) Ant. 1, (b) Ant. 2, (c) Ant. 3, and (d) Ant. 4.

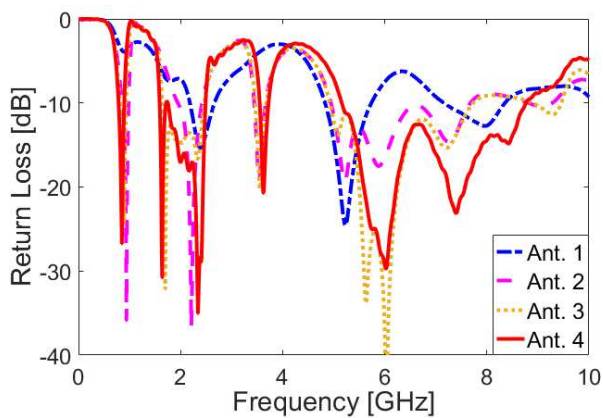


Fig. 4. Return loss characteristics for various evolutions shown in Fig. 3.

Towards a directive to validate the multi-operational working frequency to distinguish the model, the virtual current densities of the loop antenna by diverse working frequencies have been demonstrated within Fig. 5. It would be distinguished that the supreme ascending for all shapes is

identical. It can be detected that currents are vastly scattered around the L-shaped slits. The inferior resonances are accomplished by the superior L-shaped slit [17].

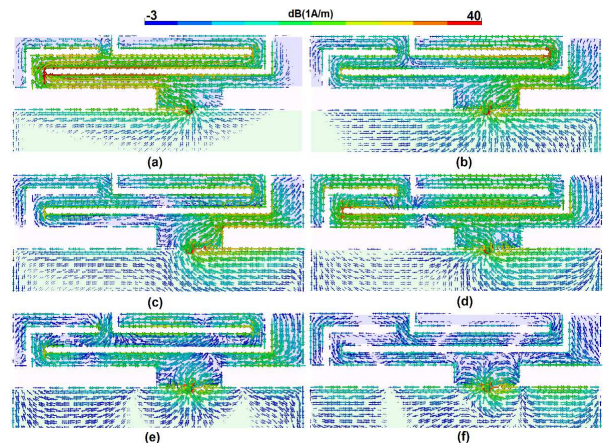


Fig. 5. Current distributions at (a) 0.9 , (b) 1.9 , (c) 2.1 , (d) 4.5 , (e) 5.5 , and (f) 7 GHz.

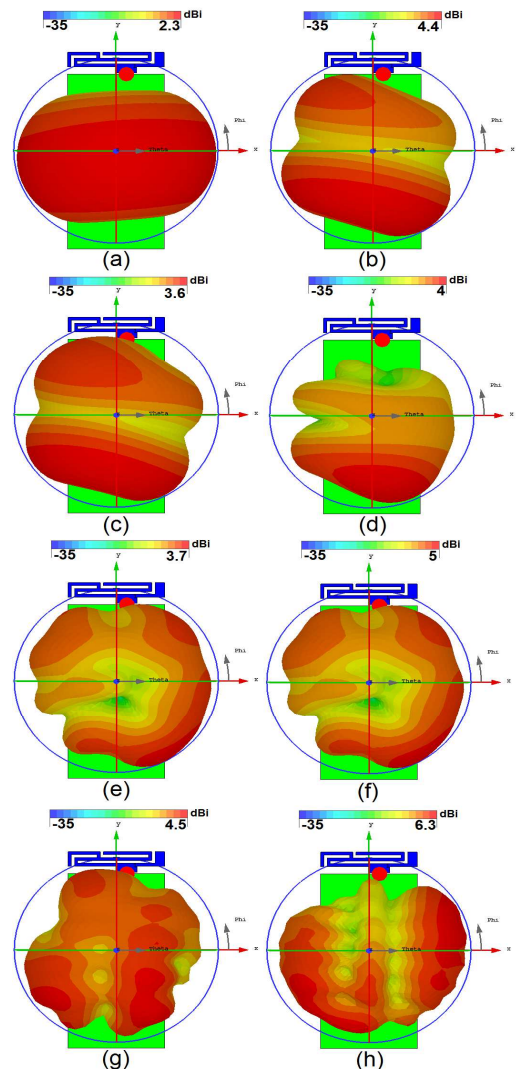


Fig. 6. 3D Radiation patterns at (a) 0.9, (b) 1.9, (c) 2.1, (d) 3.6, (e) 4, and (f) 4.5, (g) 5.5, and (h) 7 GHz.

The antenna provides sufficient maximum gains. Figure 6 presented the 3D radiations at dissimilar operational bands. It is witnessed that sufficient gain value for each radiator of the smartphone antenna design can offer. As demonstrated, the gain of the presented antenna varies from 2 to more than 6 dBi. The upper and lowest verges of the mainboard of the smartphones provide sufficient radiation coverage. The efficiency along with extreme gain characteristics of the model are demonstrated in Fig. 7. As it can be witnessed appropriate efficiencies are delivered by every single antenna. Better than 50% and 40% radiation efficiency, as well as total efficiency, are accomplished respectively for the antenna at diverse resonance frequencies [17].

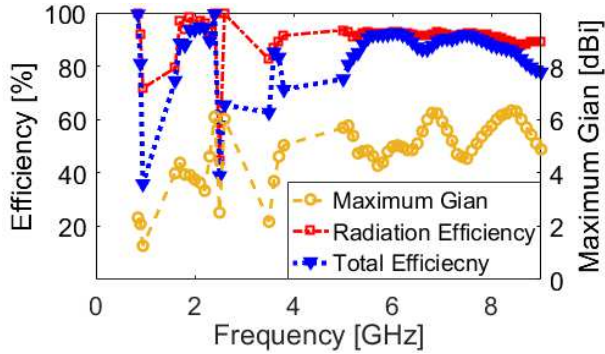


Fig. 7. Radiation and total efficiencies of the design.

III. 2×2 MIMO SMARTPHONE ANTENNA

The outline of the presented MIMO smartphone antenna is demonstrated in Fig. 8. As revealed, it is poised of two monopole radiators that have been organized at the upper and lower verges of the central board.

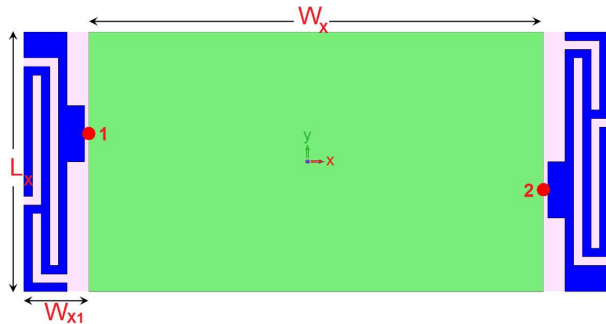


Fig. 8. 2×2 MIMO smartphone design.

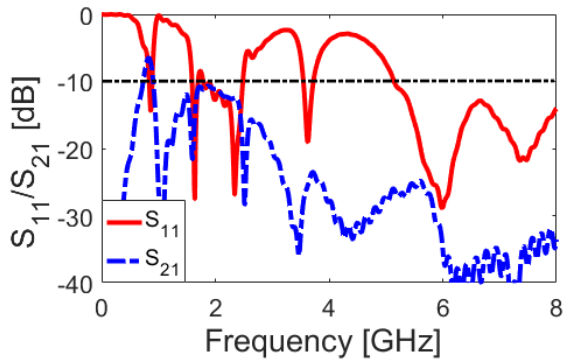


Fig. 9. S-parameters of the 2×2 MIMO smartphone design.

The S parameters (including S_{11} and S_{21}) of the projected smartphone antenna are revealed in Fig. 9. As explained, the antenna demonstrates decent S parameters at working bands covering the identical spectrums of the single-element antenna system. In addition, sufficient mutual coupling is observed in the proposed MIMO system between the two antenna elements, exclusively at the higher operational frequency bands [18]. Figure 10 shows the radiation patterns of the MIMO design for composed antenna elements at different frequencies. As seen, the presented MIMO antenna can deliver decent radiation patterns with necessary gain vales for apiece radiator. It is understood that 2.6~6.2 dBi IEEE gain distinctive is gotten for each antenna feature.

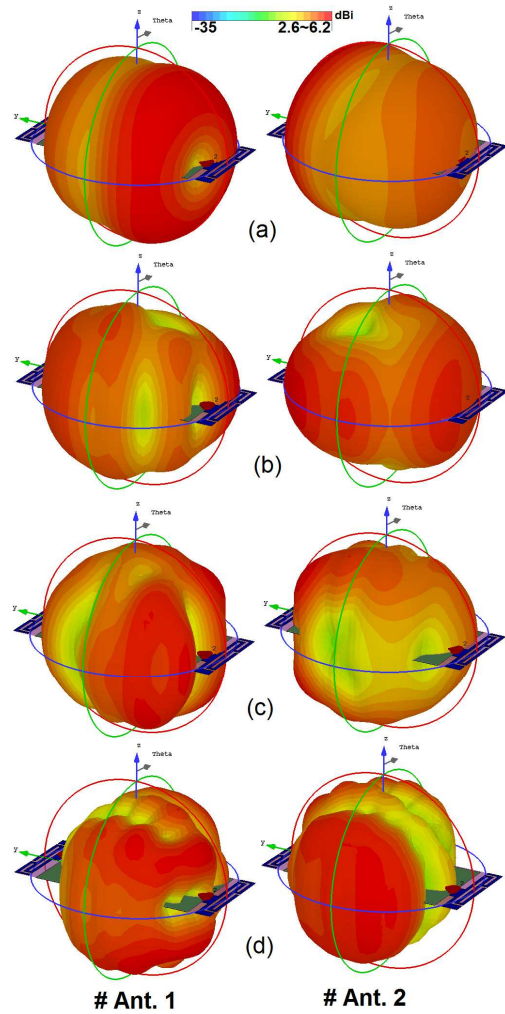


Fig. 10. Radiation patterns of the MIMO design at (a) 1.9, (b) 2.1, (c) 3.6, and (d) 7.5 GHz.

The total active reflection coefficient (TARC) and envelope correlation coefficient (ECC), features of dual elements can be considered from the S-parameters using the below equation [19-20].

$$ECC = \frac{|S_{mm}^* S_{nm} + S_{mn}^* S_{nn}|^2}{(1 - |S_{mm}|^2 - |S_{nn}|^2)(1 - |S_{nm}|^2 - |S_{mn}|^2)^*} \quad (1)$$

$$TARC = -\sqrt{\frac{(S_{mm} + S_{nn})^2 + (S_{nm} + S_{mn})^2}{2}} \quad (2)$$

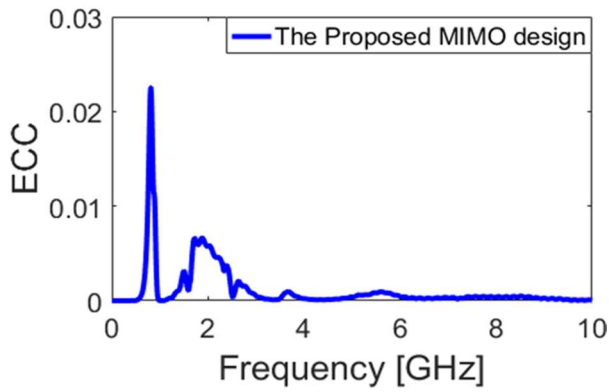


Fig. 11. ECC function of the MIMO design.

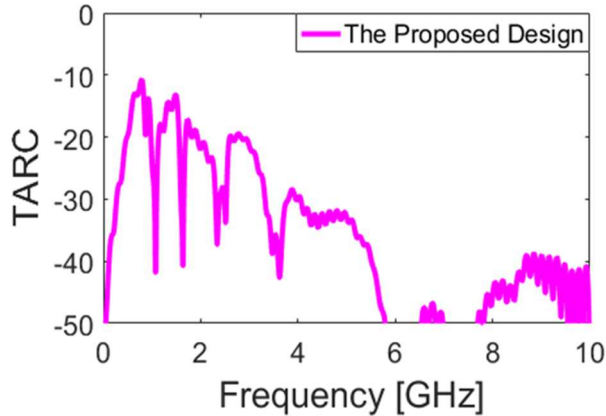


Fig. 12. TARC characteristic of the MIMO design.

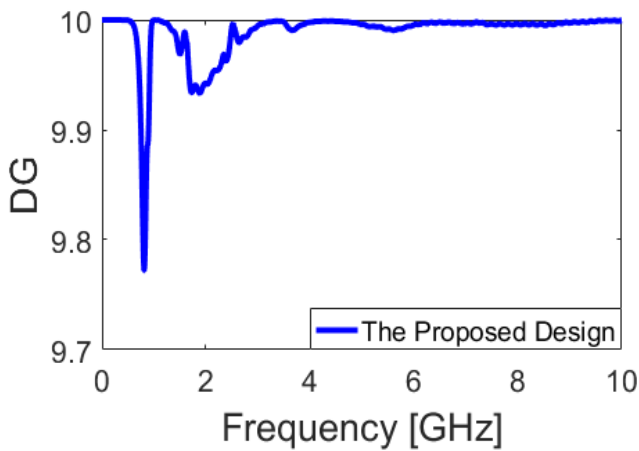


Fig. 13. DG result of the MIMO design.

As marked from Figs. 11 and 12, the ECC results are very low at the working operation bands (less than 0.025). It can be also noticed that the TARC value of the projected design is fewer than -10 dB. An additional significant parameter for the MIMO performance of the antenna is diversity gain (DG) which can be considered using the subsequent relation:

$$DG = 10\sqrt{(1 - ECC)^2} \quad (3)$$

Figure 13 shows the diversity gain utility of the presented antenna over its working band. More than 9.75 dB over the operating frequency bands is obtained.

IV. CONCLUSION

A 2×2 multi-band MIMO antenna is planned for smartphone applications. The formation of the antenna element consists of a multi-mode monopole radiator with three L-shaped slits placed at the edge of the smartphone PCB. The low-cost FR4 working substrate is used for this new design with a total dimension of $60 \times 135 \times 0.5$ mm³. For $S_{11} \leq -6$ dB, the MIMO design function within the frequency ranges of 0.79–0.92 GHz, 1.5–2.7 GHz, 3.5–3.85 GHz, and 5–9.5 GHz covering IMT, PCS, UMTS, DCS, WLAN, LTE, and X bands. The MIMO antenna delivers appropriate gains and efficiencies at different frequency bands.

REFERENCES

- [1] M. Jensen, J. Wallace, "A review of antennas and propagation for MIMO wireless communications," *IEEE Trans. Antennas Propag.*, vol. 52, pp. 2810–2824, 2004.
- [2] N. O. Parchin, *et al.*, "Dual-polarized MIMO antenna array design using miniaturized self-complementary structures for 5G smartphone applications," *EuCAP Conference*, 2019, Krakow, Poland.
- [3] Z. Zhang, "Antenna Design for Mobile Devices," Hoboken, NJ, USA: Wiley-IEEE Press, 2011.
- [4] Z. Liang, Y. Li, and Y. Long, "Multiband monopole mobile phone antenna with circular polarization for GNSS application," *IEEE Trans. Antennas Propag.*, vol. 62, pp. 1910–1917, 2014.
- [5] Y. L. Ban, *et al.*, "Low-profile printed octa-band LTE/WWAN mobile phone antenna using embedded parallel resonant structure," *IEEE Trans. Antennas Propag.*, vol. 61, pp. 3889–3894, 2013.
- [6] C. F. Ding, *et al.*, "Novel pattern-diversity-based decoupling method and its application to multielement MIMO antenna," *IEEE Trans. Antennas Propag.*, vol. 66, no. 10, pp. 4976–4985, Oct. 2018.
- [7] N. Ojaroudi, *et al.*, "An omnidirectional PIFA for downlink and uplink satellite applications in C-band," *Microwave and Optical Technology Letters*, vol. 56, pp. 2684–2686, 2014.
- [8] N. O. Parchin, *et al.*, "Dual-polarized MIMO antenna array design using miniaturized self-complementary structures for 5G smartphone applications," *EuCAP Conference*, 2019, Krakow, Poland.
- [9] N. Ojaroudi, *et al.*, "Quad-Band Planar Inverted-F Antenna (PIFA) for Wireless Communication Systems," *Progress In Electromagnetics Research Letters*, vol. 45, pp. 51–56, 2014.
- [10] M.S. Sharawi, "Printed MIMO Antenna Engineering," Artech House, Norwood, MA, USA, 2014.
- [11] N. O. Parchin, *et al.*, "8×8 MIMO antenna system with coupled-fed elements for 5G handsets," *The IET Conference on Antennas and Propagation (APC)*, 11–12 November 2019, Birmingham, UK.
- [12] A. Zhao and Z. Ren, "Size reduction of self-isolated MIMO antenna system for 5G mobile phone applications," *IEEE Antennas Wireless Propag. Lett.*, vol. 18, no. 1, pp. 152–156, Jan. 2019.
- [13] N. Ojaroudi, and N. Ghadimi, "Dual-band CPW-fed slot antenna for LTE and WiBro applications," *Microw. Opt. Technol. Lett.*, vol. 56, pp. 1013–1015, 2014.
- [14] CST Microwave Studio, ver. 2017, CST, Framingham, USA, 2017.
- [15] N. Ojaroudi Parchin, R. A. Abdalameed "A compact Vivaldi antenna array for 5G channel sounding applications," *EuCAP 2018*, 9–13 April 2018, London, UK.
- [16] N. O. Parchin, "Low-profile air-filled antenna for next-generation wireless systems," *Wireless Personal Communications*, vol. 97, pp. 3293–3300, 2017.
- [17] A. Musavand, *et al.*, "A compact UWB slot antenna with reconfigurable band-notched function for multimode applications," *ACES Journal*, vol. 13, no. 1, pp. 975–980, 2016.
- [18] N. Ojaroudi, "Microstrip monopole antenna with dual band-stop function for UWB applications," *Microw. Opt. Technol. Lett.*, vol. 56, pp. 818–822, 2014.
- [19] N. O. Parchin, *et al.*, "MIMO Antenna Systems for 5G Mobile Handsets," Lambert Academic Publishing, 2021.
- [20] N. O. Parchin, *et al.*, "Microwave/RF Components for 5G Front-End Systems," Avid Science, India, 2019.